JOURNAL OF GEOPHYSICAL RESEARCH, VOL. 112, D15205, doi:10.1029/2006JD007427, 2007

Forecast errors in dust vertical distributions over Rome (Italy): Multiple particle size representation and cloud contributions

P. Kishcha,[1] P. Alpert,[1] A. Shtivelman,[1] S. O. Krichak,[1] J. H. Joseph,[1] G. Kallos,[2] P. Katsafados,[2] C. Spyrou,[2] G. P. Gobbi,[3] F. Barnaba,[3,4] S. Nickovic,[5,6] C. Pérez,[7] and J. M. Baldasano[7,8]

Received 21 April 2006; revised 1 May 2007; accepted 22 May 2007; published 7 August 2007.

[1] In this study, forecast errors in dust vertical distributions were analyzed. This was carried out by using quantitative comparisons between dust vertical profiles retrieved from lidar measurements over Rome, Italy, performed from 2001 to 2003, and those predicted by models. Three models were used: the four-particle-size Dust Regional Atmospheric Model (DREAM), the older one-particle-size version of the SKIRON model from the University of Athens (UOA), and the pre-2006 one-particle-size Tel Aviv University (TAU) model. SKIRON and DREAM are initialized on a daily basis using the dust concentration from the previous forecast cycle, while the TAU model initialization is based on the Total Ozone Mapping Spectrometer aerosol index (TOMS AI). The quantitative comparison shows that (1) the use of four-particle-size bins in the dust modeling instead of only one-particle-size bins improves dust forecasts; (2) cloud presence could contribute to noticeable dust forecast errors in SKIRON and DREAM; and (3) as far as the TAU model is concerned, its forecast errors were mainly caused by technical problems with TOMS measurements from the Earth Probe satellite. As a result, dust forecast errors in the TAU model could be significant even under cloudless conditions. The DREAM versus lidar quantitative comparisons at different altitudes show that the model predictions are more accurate in the middle part of dust layers than in the top and bottom parts of dust layers.

Citation: Kishcha, P., et al. (2007), Forecast errors in dust vertical distributions over Rome (Italy): Multiple particle size representation and cloud contributions, *J. Geophys. Res.*, *112*, D15205, doi:10.1029/2006JD007427.

1. Introduction

[2] Three-dimensional dust forecasting over the Mediterranean is complex because of intensive cyclones responsible for dust transport from the Sahara desert [*Alpert and Ziv*, 1989; *Bergametti et al.*, 1989; *Alpert et al.*, 1990; *Moulin et al.*, 1998; *Barkan et al.*, 2004, 2005]. The intensive cyclones are often accompanied by a considerable amount of clouds. The cloud presence could be associated with some additional forecast errors in dust vertical distributions. Various interactions between dust and clouds are not really incorporated in full measure in current numerical weather and climate prediction models, because, for the most part, they are not yet fully understood [*Kaufman et al.*, 2002; *Rosenfeld*, 2002; *Ramanathan et al.*, 2001]. Nevertheless, for the past decade, several three-dimensional models for simulation and prediction of the atmospheric dust cycle have been developed [*Nickovic and Dobricic*, 1996; *Kallos et al.*, 1997; *Nickovic et al.*, 2001; *Nickovic*, 2005; *Kallos et al.*, 2006]. Moreover, experimental versions of the regional dust model with radiative effects of dust have been recently constructed [*Krichak et al.*, 2003; *Nickovic et al.*, 2004; *Pérez et al.*, 2006a].

[3] In order to assess present-day and future research in dust modeling we need to pay attention to the existing background in this field. The current study is devoted to a comparative analysis of 24-hour forecast errors in dust vertical distributions for dust prediction systems operating in the Mediterranean region. It is worth noting that all those systems have been in daily use for several years. Therefore the results of this analysis could be indicative of the reliability of their dust forecasts over the past decade.

[1]Department of Geophysics and Planetary Sciences, Tel Aviv University, Tel Aviv, Israel.
[2]Division of Environment, School of Physics, University of Athens, Athens, Greece.
[3]Istituto di Scienze dell'Atmosfera e del Clima, Italian National Research Council (CNR), Rome, Italy.
[4]Now at Climate Change Unit, Institute for Environment and Sustainability, Joint Research Centre (JRC), European Commission, Ispra, Italy.
[5]Euro-Mediterranean Centre on Insular Coastal Dynamics, University of Malta, Valletta, Malta.
[6]Now at Atmospheric Research and Environment Programme, World Meteorological Organization, Geneva, Switzerland.
[7]Earth Sciences Department, Barcelona Supercomputing Center, Barcelona, Spain.
[8]Also at Environmental Modeling Laboratory, Technical University of Catalonia, 08028 Barcelona, Spain.

0148-0227/07/2006JD007427$09.00

Table 1. Particle Size Bins, Domains, Horizontal and Vertical Resolution, Dust Source Data, and Approach to Dust Initialization in the Models Under Consideration[a]

MODEL Size Bins, Effective Radii, μm	Domain	Resolution		Dust Initialization	Dust Source Data, Resolution
		Horizontal, degrees	Vertical, Levels Heights, m		
DREAM 4 (0.7, 6.1, 18.0, 38.0)	15N–50N 20W–45E	0.30	24 (86–15022)	previous forecast	USGS (30 s) and Olson data (10 min)
SKIRON 1 (2)	16N–54N 12W–39E	0.24	32 (124–15480)	previous forecast	USGS (30 s) and Olson data (10 min)
TAU 1 (2)	0–50N 50W–50E	0.50	32 (124–15480)	TOMS indices	*Ginoux et al.*'s [2001] method

[a]TAU: Tel Aviv University. TOMS: Total Ozone Mapping Spectrometer.

[4] In order to evaluate the model capabilities for providing reliable forecasts of 3-D dust distributions in the atmosphere, we used the dust forecasts of three different forecasting systems: the four-particle-size Dust Regional Atmospheric Model (DREAM) [*Nickovic et al.*, 2001], the pre-2006 one-particle-size Tel Aviv University (TAU) dust prediction system [*Alpert et al.*, 2002], and the older one-particle-size version of the SKIRON model of the University of Athens (UOA) [*Kallos et al.*, 1997]. These three model versions have their origin in the same predecessors described by *Nickovic and Dobricic* [1996], *Kallos et al.* [1997], and *Nickovic et al.* [1997], with various components upgraded afterward. The dust forecasts were compared against lidar remote soundings over Rome, Italy (41.8°N, 12.6°E) performed over the 3-year period 2001–2003, for the high dust activity season over the Mediterranean from March to June.

2. Dust Prediction System

[5] The older version of SKIRON forecasting system of the University of Athens, used in this study, includes a dust module with the one-particle-size representation of dust aerosol [*Kallos et al.*, 1997]. This SKIRON system has been in operational use since 1998 providing 72-hour weather and dust forecasts for the Mediterranean region. Dust is driven by the hydrostatic NCEP/Eta model. The SKIRON system covers a domain including the Mediterranean Sea, Europe, North Africa and Middle East. In the vertical, 32 levels are used from the ground to the model top (15,500 m). In the horizontal, a grid size of 0.25 degrees is used (Table 1).

[6] The system includes packages for dust initialization, transport, and wet/dry deposition, developed initially by *Nickovic and Dobricic* [1996] and further developed within the framework of the Mediterranean Dust Experiment (MEDUSE) EU project by the University of Athens Atmospheric Modeling and Weather Forecasting Group [*Kallos et al.*, 1997; *Nickovic et al.*, 1997; *Papadopoulos et al.*, 1997]. The dust module is dynamically coupled with the atmospheric model; therefore at each time step the prognostic atmospheric and hydrological conditions are used to calculate the effective rates of the injected dust concentration on the basis of the viscous/turbulent mixing, shear-free convection-diffusion, and soil moisture. Special care was taken to define as accurately as possible the dust productive areas since soil properties (soil structure, soil wetness, vegetation cover) dictate the dust quantity that may be available when the turbulent state of the surface atmosphere triggers its injection into the atmosphere. The specification of the model dust sources and the calculation of dust-related processes are obtained from high-resolution data sets of vegetation and soil texture types. In particular, this older version of SKIRON used the 30-sec resolution US Geological Survey (USGS) topography and land use data sets as the basis for the identification of dust sources, in combination with the Olson World Ecosystem Data classification of 10-min resolution [*Papadopoulos*, 2001; *Nickovic et al.*, 2001]. For soil texture distribution, the UNEP/FAO data set was applied after its conversion from soil type to soil textural ZOBLER classes [*Papadopoulos et al.*, 1997]. The entire source area scheme used was developed by *Papadopoulos* [2001], and is the same as in the newer version of the SKIRON system [*Kallos et al.*, 2006]. The dust is considered as a passive substance; that is, no dust feedback effects are included in the radiation transfer calculations. It should be mentioned that a new version of SKIRON has been developed at the University of Athens, which includes a dust module with the four-particle-size representation of dust aerosol [*Nickovic et al.*, 2001; *Kallos et al.*, 2006]. Being in operational use since January 2003, it has the same elements as DREAM described below, since their development was done in the framework of the SKIRON and MEDUSE and later the ADIOS projects.

[7] The one-particle-size SKIRON system, after modification, was put into operation and has been used for short-term dust predictions at Tel Aviv University from November 2000 until the end of 2005 [*Alpert et al.*, 2002]. This model is called hereafter the TAU model. Several modifications were made to the model including development of a new dust initialization procedure, determination of the dust sources employing *Ginoux et al.*'s [2001] method, and expansion of the forecast area to include the Atlantic Ocean. These improvements were undertaken in order to support the joint Israeli-American Mediterranean Dust Experiment (MEIDEX). The model domain is 0–50°N, 50°W–50°E. The model has a horizontal resolution of 0.5 degrees and 32 vertical levels (Table 1). Dust forecasts are initialized with the aid of the Total Ozone Mapping Spectrometer aerosol index (TOMS AI) measurements [*Alpert et al.*, 2002]. The initial dust vertical distribution over each grid point, within the model domain, is determined according to the value of TOMS indices with four categories of model-calculated averaged dust profiles over the Mediterranean and among four other profiles over North Africa. The dust component is based on a single particle size bin with radius of 2 microns. Further details are given by *Alpert et al.* [2002].

[8] The four-particle-size DREAM model incorporates the state-of-the-art parameterizations of all the major phases of atmospheric dust life such as production, diffusion, advection and removal [*Nickovic et al.*, 2001]. In DREAM, the emission parameterization combines the flux scheme of *Shao et al.* [1993] and viscous sublayer model of *Janjic* [1994]. Its dust module includes effects of the particle size distribution on aerosol dispersion. In particular, special attention was made in order to properly parameterize the dust production phase. Dust productive areas in the model are specified similarly to those in the SKIRON model, by using the 30-sec resolution USGS topography and land use data sets as the basis for the identification of dust sources. For each soil texture class the fractions of clay, small silt, large silt and sand are estimated with four particle size radii of 0.7, 6.1, 18.0, and 38 microns, respectively. In DREAM, the dust cycle is described by a set of K-independent Euler-type concentration equations allowing no interparticle interactions, where K = 4 indicates the number of particle size class. The area covered by the model is 20°W to 45°E and 15°N to 50°N. The model has a horizontal resolution of 0.3 degrees and 24 vertical levels between the surface and ~15000 m. Experimental versions of the model with eight-particle-size bins and dust treated as a radiatively active aerosol have been recently developed [*Nickovic et al.*, 2004; *Nickovic*, 2005; *Pérez et al.*, 2006a; *Pérez et al.*, 2006b].

[9] To compare the dust forecast with lidar-derived volume profiles, modeled mass concentration profiles over Rome were divided by dust density, assumed as 2.5 g/cm^3, in agreement with the majority of other dust models [e.g., *Kinne et al.*, 2003, Table 4].

3. Lidar Data

[10] Lidar measurements employed in this study were collected by an elastic backscatter, single-wavelength, polarization-sensitive lidar system (VELIS), operational since February 2001 at the ISAC laboratories (41.84N–12.64E, 130 m asl) at the outskirts of Rome, Italy [*Gobbi et al.*, 2004]. Measurements were carried out daily at nonsynchronous times between 7 am and 7 pm (UTC). A thorough description of the VELIS system and lidar signal analysis can be found in the work of *Gobbi et al.* [2002, 2003]. We just recall here that the VELIS lidar radiation source is a frequency-doubled Nd:YAG laser, emitting plane-polarized pulses at 532 nm. The energy and repetition rate of laser pulses are generally set as 30 mJ and 10 Hz, respectively. The system set up allows collecting the complete tropospheric backscatter (β) profile between 300 m and 14 km from the ground. To infer particle shape, the system is equipped with two receiving channels to record the light backscattered on both the parallel ($\beta_{//}$) and perpendicular ($\beta_{\perp}$) polarization planes with respect to the laser one. This gives a measure of the depolarization, D = ($\beta_{\perp}/\beta_{//}$). Our observations show that gas molecules and spherical particles (which do not/slightly change the laser polarization plane) give D ≈ 1–2%. Conversely, nonspherical particles change the polarization plane of the laser light, giving higher depolarization values. Typical D values in the presence of desert dust range between 10–45%, depending on the relative impact of nonspherical particles on the total (aerosol + molecules) backscattered signal [e.g., *Gobbi et al.*, 2002]. A convenient way to evaluate the aerosol load by lidar is through the backscatter ratio R = ($\beta_a + \beta_m$)/β_m, where β_a and β_m are the aerosol and the molecular backscatter, respectively (R = 1 thus indicating an aerosol-free atmosphere, with increasing R for increasing aerosol contribution). The combination of both the backscatter ratio (R) and the depolarization information is therefore used to distinguish between dust (typically D > 10% and correlated behavior of D and R) and non–dust conditions (typically D < 10%, anticorrelated behavior of D and R).

[11] Lidar profiles are obtained as 10-min averages and their vertical resolution is 37.5 m. The *Barnaba and Gobbi* [2001] approach was used in the current study to derive height-resolved dust volumes from lidar measurements of backscatter. A validation of the lidar-estimated dust volume with respect to in situ observations is given by *Gobbi et al.* [2003]. In particular, comparisons between lidar data and in situ dust volume measurements showed a slight (−1%) systematic lidar tendency to underestimate desert dust volume, and an average agreement within ±20%. Those comparisons were performed in the near range portion of the lidar trace (altitudes <500 m), where the lidar error is generally low. Nonetheless, a similar 20% mean accuracy of the lidar-derived volume is expected up to about 4 km, region in which the VELIS random error stays of the order of 1%. On the other hand, VELIS typically shows an additional random error to affect the farther ranges (of the order of ~8% at 4–6 km and ~30% at 6–8 km), translating into an overall mean accuracy of the lidar-derived particle volume in these regions of 30% and 50%, respectively.

[12] A database of 34 days was selected for the lidar versus model comparison with further details given by *Kishcha et al.* [2005]. Since this study was aimed at checking the quality of dust forecasts available at 12 UTC, the lidar dust profiles closest to 12 UTC were selected for the analysis.

4. Results

4.1. Quantitative Intercomparison

[13] The correspondence between model data and lidar measurements over Rome is evaluated by means of scatterplots with lidar-derived versus model-simulated dust volumes (Figure 1). The bisector curves, shown in the plot, indicate ideally accurate forecasts; that is, the points on or close to the bisector represent the best correspondence between the model-simulated data and the lidar ones. The root-mean-square intervals of deviations of points from the bisector (the dashed lines in Figure 1) can be used in order to characterize the range of forecast accuracy.

4.1.1. TAU Model Versus Lidar

[14] The distribution of points in the scatterplot in Figure 1a reveals that the model results vary between $0.04 \cdot 10^{-12}$ cm^3/cm^3 and $9.05 \cdot 10^{-12}$, whereas the lidar data are between the lower detection limit of $3.62 \cdot 10^{-12}$ and $163.0 \cdot 10^{-12}$. Almost all points to the right of the vertical line (Vmod ~ $1 \cdot 10^{-12}$ cm^3/cm^3 are located within the root-mean-square interval. Alternatively, below the $1 \cdot 10^{-12}$ cm^3/cm^3 threshold (i.e., the left of this vertical line) all points are located outside the root-mean-square interval. From the model simulations point of view, this unambiguously means that

predicted dust volumes (Vmod, along the *x axis*) lower than $1 \cdot 10^{-12}$ cm^3/cm^3 are not reliable [*Kishcha et al.*, 2005].

[15] Overall, for the 34 days under consideration, the correlation r = 0.47 between lidar and model derived dust volume was obtained (Table 2). The correlation is statistically significant within the 0.05 level. In a previous paper [*Kishcha et al.*, 2005], attention was paid to the fact that inaccurate forecasts were associated with cloudiness, over the area where the initial 3-D dust distribution had been obtained (with the aid of TOMS indices on the day previous to the forecast). Earth Probe Total Ozone Mapping Spectrometer reflectivity measurements (see http://daac.gsfc.nasa.gov) were used in order to identify cloudy conditions for all points in the above discussed scatterplots of Figure 1a. Averaged reflectivity of less than 20% over the area, where dust was initialized 24 hours before the forecast time, was found to correspond mainly to acceptable forecast points. The area, where dust was initialized, is defined by the rectangular area around the starting points of 24-hour back trajectories. However, as found in the current study for the TAU model, the forecast errors could be significant even in cloudless conditions. In particular, for 22 days with low cloud presence (averaged TOMS reflectivity less than 20%), over the area where the dust originated, the correlation is rather low (r = 0.44). This is mainly caused by technical problems with TOMS measurements in accordance with NASA announcements (http://daac.gsfc.nasa.gov/data/data set/TOMS). These problems became more severe in the recent years and led NASA to the decision to stop generating TOMS aerosol indices by the end of 2005. It seems that earlier runs (1999–2001) with TOMS AI, as reported by *Alpert et al.* [2002], yielded a significant improvement over the alternative dust initialization.

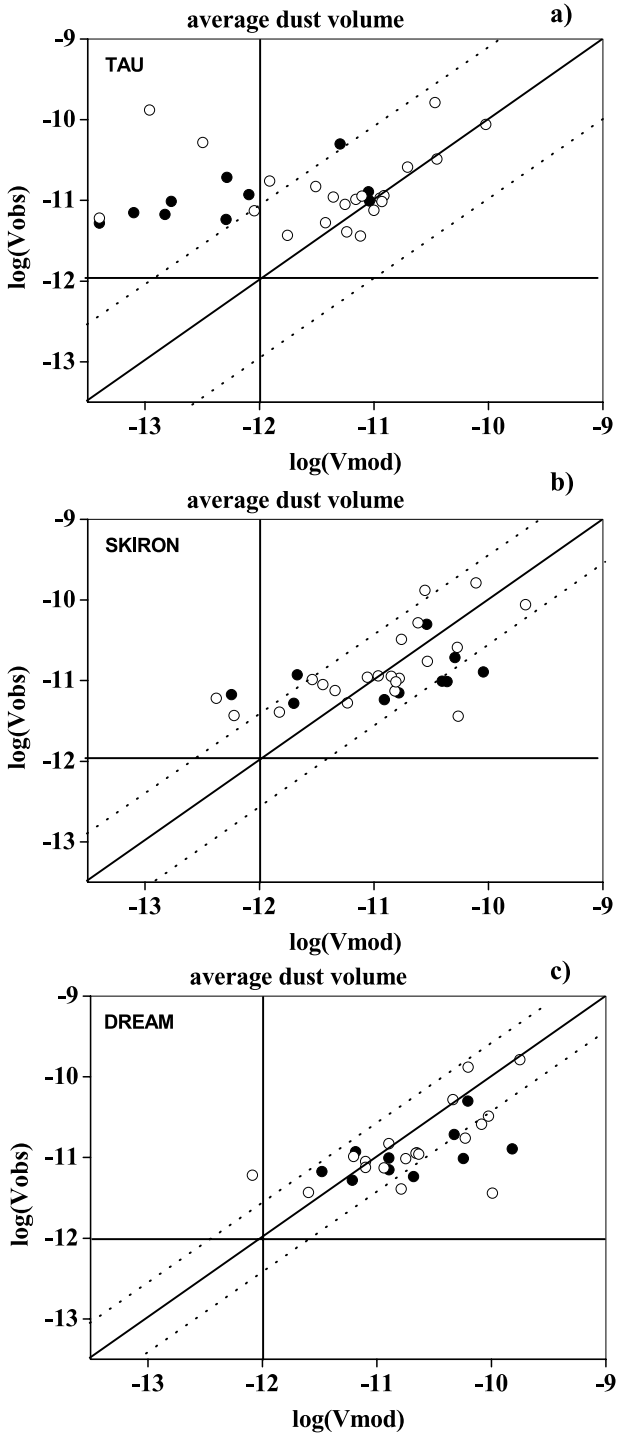

Figure 1. Scatterplots between the common logarithm of model-simulated dust volumes (Vmod) (cm^3/cm^3) over Rome, averaged within the dust layer, and the ones retrieved from lidar soundings (Vobs) for 34 days under consideration. (a) Tel Aviv University (TAU) model, (b) SKIRON, (c) Dust Regional Atmospheric Model (DREAM). Dashed lines show the root-mean-square intervals of deviations from the bisector. Open circles correspond to 22 days with low cloud presence (averaged Total Ozone Mapping Spectrometer (TOMS) reflectivity less than 20%) over the area where the dust originated. Solid circles correspond to 10 days with cloudiness exceeding 20% over the area where the dust originated. Horizontal solid lines, intersecting the vertical axis (lidar data) at 1×10^{-12} cm^3/cm^3, correspond to the minimum dust volume detected by the lidar. Vertical solid lines, intersecting the horizontal axis (model data) at 1×10^{-12} cm^3/cm^3, correspond to the threshold of trustworthy dust forecasts.

4.1.2. SKIRON Versus Lidar

[16] Shown in Figure 1b, the distribution of points in the scatterplot reveals that the SKIRON model results vary between $0.42 \cdot 10^{-12}$ cm^3/cm^3 and $211.16 \cdot 10^{-12}$ cm^3/cm^3. The SKIRON data correspond better to the lidar ones, as compared with the TAU model results. In particular, the root-mean-square interval is half as wide as that for the TAU data, indicating that, in the scatterplot, the deviation of points from the bisector is smaller. Only a few points are located below the threshold of trustworthy dust forecasts (i.e., to the left of the vertical line 1×10^{-12} cm^3/cm^3).

[17] As shown in Table 2, the correlation r = 0.49 was found for all 34 days under consideration. However, it was surprising that for 22 days with low or without cloud presence over the area, where dust was initialized, the model-lidar correspondence is noticeably better, a higher correlation (r = 0.54) was found.

Table 2. Correlation Between Lidar Data and 24-Hour Model-Predicted Dust Volumes, Averaged Within the Dust Layer[a]

Model	All 34 days	22 days With Low Cloud Presence
Four-particle-size DREAM	0.60	0.71
One-particle-size SKIRON	0.49	0.54
One-particle-size TAU	0.47	0.44

[a]DREAM: Dust Regional Atmospheric Model.

4.1.3. DREAM Versus Lidar

[18] Shown in Figure 1c, the distribution of points in the scatterplot indicates that the DREAM data better correspond to the lidar ones compared with other two models. The DREAM model results vary between $0.82 \cdot 10^{-12}$ cm^3/cm^3 and $177.04 \cdot 10^{-12}$ cm^3/cm^3. Only one point is located to the left of the vertical line 1×10^{-12} cm^3/cm^3. The majority of points to the right of that vertical line are located within the root-mean-square interval, which is the narrowest one among those for three models under consideration, indicating that DREAM produces dust forecasts of higher accuracy than other models.

[19] This is supported by higher correlation (r = 0.60) for all 34 days under consideration. It is noticeable that for the days with low or without cloud presence over the area, where the dust originated, the model-lidar correspondence is distinctly better, a higher correlation (r = 0.71) was found (Table 2).

4.2. Statistical Histograms of Forecast Errors

[20] An analysis of statistical distributions of forecast mean errors allows the clarification of the difference between the three dust prediction systems under investigation. To this end, statistical histograms of 24-hour forecast errors for averaged dust volume within the dust layer over Rome were constructed, as shown in Figure 2. The forecast mean error was defined as the difference between the common logarithm of lidar-derived dust volume and the one simulated by the model. Consequently, positive errors mean underestimating of lidar data by the model, while negative ones mean overestimating. Different histograms are analyzed in Figure 2: (1) for all the 34 days in question (Figure 2a), (2) only for the 22 days with low cloud presence (Figure 2b), and (3) for the 10 days with cloudiness exceeding 20%, as characterized by the averaged TOMS reflectivity over the area where the dust originated (Figure 2c).

[21] The histograms in Figure 2a reveal the following characteristic features of forecast error distributions: (1) Maxima of the histograms are close to zero, meaning that, on average, both SKIRON and DREAM produce acceptable forecasts. (2) However, the TAU model errors are spread over a wide range, indicating that the TAU model predictions tend to underestimate lidar data; the errors are mainly positive. (3) The error distribution for the SKIRON model is more symmetric than that for DREAM; DREAM tends to overestimate lidar data.

[22] Figure 2b demonstrates that, for days with low or without cloud presence, forecast errors are spread over a narrower range. This highlights the fact that these cases without clouds are mainly associated with dust forecasts of higher accuracy. As for the TAU model, forecast errors are spread over a wider range because of inaccurate TOMS data.

[23] In contrast, as shown in Figure 2c for cloudy days, for all models errors are spread over a wider range, pointing to that these cases are frequently associated with dust forecasts of lower accuracy. The TAU model errors shift to positive values (underestimation), while those for DREAM and SKIRON shift to negative values (overestimation).

4.3. DREAM Versus Lidar Comparisons at Different Altitudes

[24] DREAM, because of its proven capability for reliable forecasting, was selected for specific evaluation of dust forecast at different altitudes. In Figure 3 (top) 269 points were used for DREAM versus lidar intercomparisons at different altitudes, of which 89, 138 and 42 points belong to the top (above 3.5 km), middle (between 1.5 and 3.5 km) and bottom (below 1.5 km) parts of dust layers, respectively. One can see that nearly all points, located to the left of the threshold of trustworthy dust forecast (Vmod $\sim 1 \times 10^{-12}$ cm^3/cm^3, the vertical line in Figure 3, top), are crosses. This fact indicates that DREAM sometimes produced less reliable forecasts in the top part of dust layers. In percentage terms, 35% of points above 3.5 km, 29% of points below 1.5 km, and only 24% of points between 1.5 and 3.5 km were estimated to be located outside of the root-mean-square interval. Therefore DREAM produced more accurate forecasts in the middle part of dust layers than in the top and bottom parts of dust layers.

[25] These distinctive features of the DREAM forecasts for different parts of the dust layer are supported by the analysis of statistical distributions of 24-hour forecast errors, as shown in Figure 3, bottom. We see that, for points between 1.5 and 3.5 km within the dust layer, a considerable maximum is observed close to zero, meaning acceptable forecasts. However, at altitudes higher than 3.5 km within the dust layer, forecast errors are spread over a wide range. This indicates that the model sometimes underestimates dust at the top part of the dust layer; where significant positive errors were estimated. This result is in line with that obtained by *Kishcha et al.* [2005] for the TAU model predictions.

4.4. Examples of Model Versus Lidar Comparisons

[26] Model-lidar comparisons over Rome for two days, 17 May 2001 and 12 May 2003, were discussed by *Kishcha et al.* [2005] as the examples of accurate and inaccurate forecasts produced by the TAU model. It was interesting to evaluate the predictions of DREAM and SKIRON for the same dust events (Figure 4).

[27] For both these days (17 May 2001 and 12 May 2003), the lidar-derived dust volumes, averaged within the dust layer over Rome, are approximately the same (7.03×10^{-12} cm^3/cm^3 and 7.54×10^{-12} cm^3/cm^3, respectively). The TAU-simulated averaged dust volumes differ significantly (0.08×10^{-12} cm^3/cm^3 and 10.03×10^{-12} cm^3/cm^3), while the SKIRON-simulated figures (16.53×10^{-12} cm^3/cm^3 and 4.58×10^{-12} cm^3/cm^3) and the DREAM-simulated ones (12.76×10^{-12} cm^3/cm^3 and 7.96×10^{-12} cm^3/cm^3) corresponded much better to the lidar data for both days under consideration. It is worth noting that, for the dust

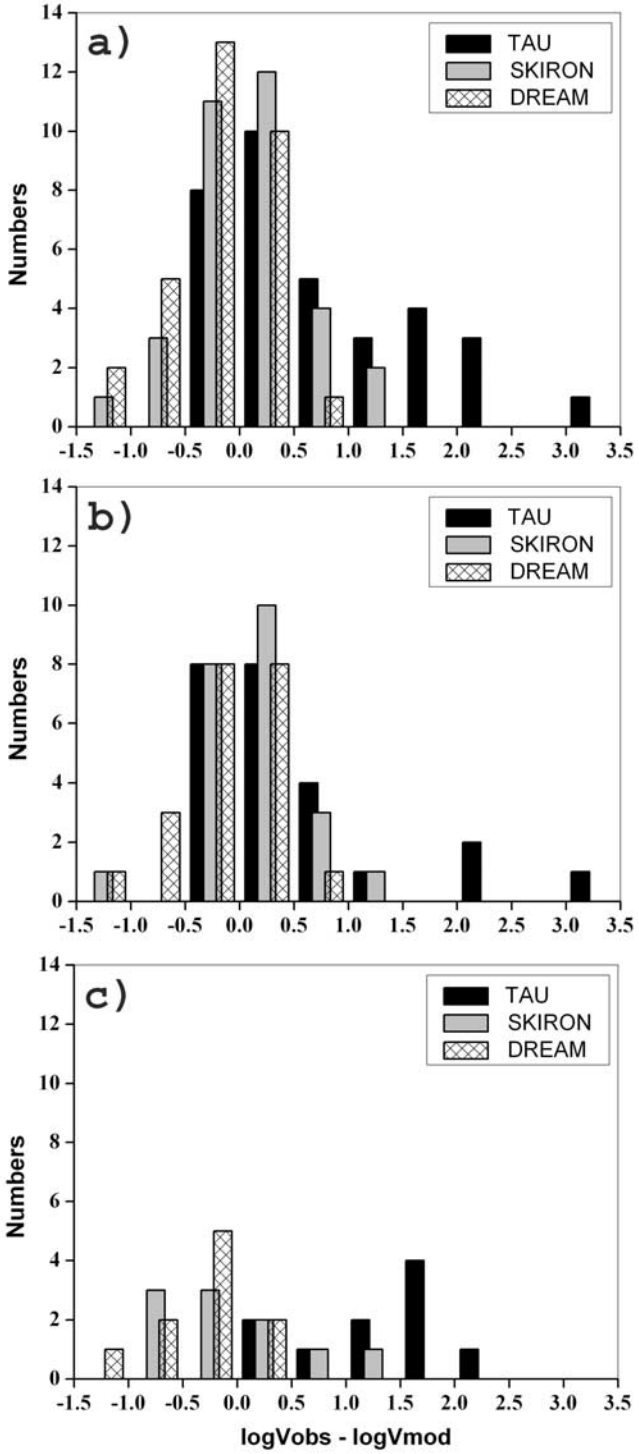

Figure 2. Statistical distributions of 24-hour forecast errors for model-simulated dust volume over Rome (averaged dust volume within the dust layer): (a) for all the 34 days under investigation, (b) for the 22 days with low cloudiness less than 20%, and (c) for the 10 days with cloudiness exceeding 20% over the area where the dust originated.

intrusion on 17 May 2001 when the TAU model significantly underestimated lidar data, both DREAM and SKIRON slightly overestimated lidar data. This is also seen in Figure 4a, displaying dust volume profiles for that dust event. This example highlights the fact that incorrect TOMS indices could result in significant forecast errors.

[28] Figure 4c presents the Sea-WIFS image of the Mediterranean area for 16 May 2001, the day previous to the dust intrusions over Rome on 17 May 2001. One can see clouds between North Africa and Italy, which cover the area (shown by the rectangle in Figure 4e), built around the endpoints of 24-hour back trajectories. The back trajectories have been calculated by using the HYSPLIT model (R. R. Draxler and G. D. Rolph, Hybrid Single-Particle Lagrangian Integrated Trajectory (HYSPLIT) Model access via NOAA ARL READY Website, 2003, NOAA Air Resources Laboratory, Silver Spring, Maryland, available at http://www.arl.noaa.gov/ready/hysplit4.html). Initialized in this area, the model-simulated dust would subsequently be transported over Rome. The starting points of 24-hour back trajectories were taken at the bottom, middle, and top heights of the lidar-measured dust layer over Rome on the forecast day. According to the Earth Probe Total Ozone Mapping Spectrometer measurements, reflectivity values greater than 20% were observed in the area under discussion (Figure 4g). In contrast, the dust forecast on 12 May 2003 was accompanied by cloudless conditions (Figure 4d) and low TOMS reflectivity (less than 20% in Figure 4h) over the rectangular area (Figure 4f), where dust was initialized 24 hours before the forecast time.

5. Conclusions

[29] The current study was devoted to the comparative analysis of model capabilities for providing reliable forecasts of dust vertical distribution in the atmosphere. This was carried out by using quantitative comparisons between dust vertical profiles retrieved from lidar measurements over Rome and those predicted by three models. Note that we used the existing configurations of dust prediction systems for comparisons. As mentioned above, these models have much in common; however, there are some differences among them, as seen in Table 1. The differences have been taken into account in our analysis, as listed below.

[30] 1. DREAM and SKIRON have approximately the same domains, horizontal resolution and approach to dust initialization. Moreover, both DREAM and SKIRON use the same data set (Olson World Ecosystem Data) to define the dust production areas. The main difference between DREAM and SKIRON is their approach to the dust particle size bins used. In particular, DREAM uses four particle size bins (0.7, 6.1, 18.0 and 38 microns), while SKIRON uses only one bin (2 microns). Therefore a comparative analysis of DREAM and SKIRON dust vertical profiles over Rome allows us to evaluate the advantage of multiple particle representation in dust forecasting.

[31] 2. TAU and SKIRON have the same single size bin. However, they have different domains, horizontal resolution, dust source data and approach to dust initialization (Table 1). As mentioned above, TAU used TOMS indices to determine the initial 3-D dust distribution in the model. In accordance with the aforementioned NASA announcements, TOMS indices became unreliable because of technical problems onboard the Earth Probe satellite. P. Kiss et al. (Early calibration problems detected in TOMS Earth Probe aerosol signal, submitted to *Geophysical Research*

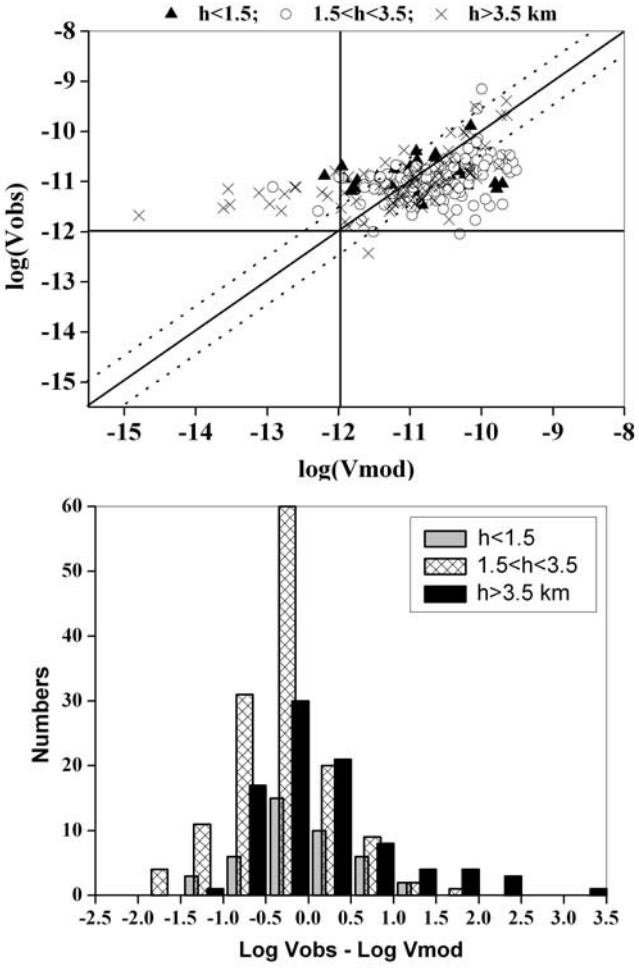

Figure 3. (top) Scatterplot between the common logarithm of the DREAM-simulated dust volumes over Rome at different altitudes along the dust profiles, and those retrieved from lidar soundings (269 points). Triangles designate dust volume at altitudes below 1.5 km (42 points); circles designate dust volume at atlitudes between 1.5 and 3.5 km (138 points); and crosses designate dust volume at altitudes above 3.5 km (89 points). Designations of dashed and solid lines are the same as in Figure 1. (bottom) Statistical distributions of 24-hour forecast errors for the DREAM-simulated dust volume. Gray shading represents forecast errors at altitudes below 1.5 km; cross-hatch pattern represents forecast errors at altitudes between 1.5 and 3.5 km; and black shading represents forecast errors at altitudes above 3.5 km.

Letters, 2006), who gave a convincing description of the degradation in the TOMS data, corroborated this fact. Incorrect TOMS indices could have resulted in significant errors in predicted dust vertical profiles over Rome, even over a hundred percent in the underestimation of lidar data (Figure 2 and Figure 4a). In contrast, the differences in domains and horizontal resolutions could be responsible only for relatively small discrepancies in predicted dust volume, averaged within the dust layers (estimated 10–20%, either positive or negative). As far as the difference in dust source data is concerned, it is well to bear in mind that dust sources in the Sahara desert are located far away from Rome (>1000–2000 km, along air mass trajectories) where the lidar measurements were taken, consequently, the difference in distributions of Saharan dust sources could only slightly affect dust vertical distributions there. Therefore we assume that the differences between the dust vertical profiles predicted by SKIRON and those predicted by the TAU model can be attributed mainly to unreliable TOMS indices.

[32] Our comparative analysis of model versus lidar correspondence highlights the following:

[33] 1. The model versus lidar comparison clearly shows the advantage of using multiple particle size representation in dust modeling. The use of four particle size bins in the dust model DREAM (and evidently in the newer four-particle-size version of SKIRON), instead of the use of only one size bins in the older one-particle-size version of SKIRON, improves dust forecasts. The correlation between model and lidar data for all 34 days under consideration is equal to 0.60 for DREAM against 0.49 for the one-particle-size SKIRON model. This is also supported by the correlation estimates for cloudless conditions.

[34] 2. For cases with low, or without cloud presence over the area where the dust originated, a higher correlation was found: 0.71 for DREAM and 0.54 for SKIRON. This highlights that cloud presence could contribute to additional dust forecast errors in SKIRON and DREAM. Two possible reasons are suggested:

[35] 1. Weather forecast errors in cloud position, amount, and structure could affect the radiation balance over the dust sources. This implies additional errors in dust emission because of its link with the sensible heat flux over dust sources [*Pérez et al.*, 2006a]. In particular, a smaller outgoing sensible turbulent heat flux reduces both dust emission and the turbulent momentum transfer from the atmosphere.

[36] 2. Nonincluded dust-radiation and dust-cloud interactions in the modeling systems could result in the forecast of lower accuracy in the presence of clouds. Recently, *Pérez et al.* [2006a] introduced the dust radiative effect into DREAM, outlining its critical influence on the weather and dust forecasts produced by the model.

[37] The present study, however, has the following limitations: (1) uncertainties in the lidar data, (2) only one lidar station (Rome) was used in the validation of the models, and (3) a limited number of dust episodes were analyzed. For these reasons the hypotheses aforementioned should be explored in detail, using a larger set of episodes and measurements.

[38] As for the pre-2006 TAU model, our findings highlight the fact that, for days with low or without cloud presence, the TAU dust forecasts were quite accurate for the most part, in contrast to those for days with cloudiness (Figure 1a). Note that all TAU model dust predictions have been produced under the same dust source data. The fact, that TAU dust forecasts were mainly accurate in the days without cloud presence and less accurate in the days with cloud presence, indicates that the main reason for inaccurate forecasts was the TOMS initialization and not the distribution of dust sources.

[39] For some infrequent dust events, however, the TOMS problems took place even in the absence of cloudiness. Therefore as shown in Figure 1a for the TAU model,

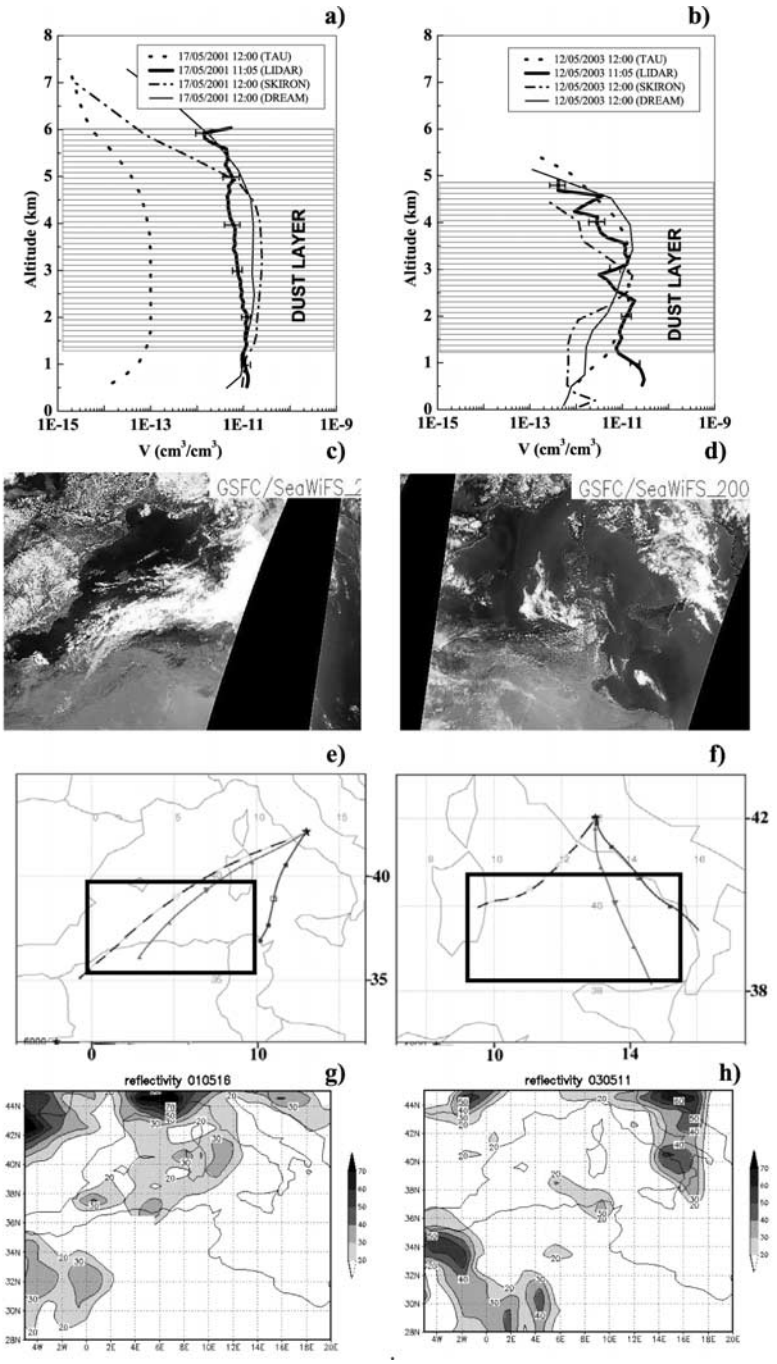

Figure 4. (a and b) Dust volume profiles over Rome during Saharan dust intrusions on 17 May 2001 and 12 May 2003, respectively. Bold solid lines correspond to the lidar data, thin solid lines correspond to the DREAM data, dash-dotted lines correspond to the SKIRON data, and dotted lines correspond to the TAU model data. Error bars on the measured lidar data are shown by the horizontal lines. (c and d) SeaWIFS images of cloudiness over the Mediterranean area. (e and f) Twenty-four-hour air mass back trajectories starting over Rome together with (g and h) horizontal distributions of reflectivity based on the measurements made by the Earth Probe Total Ozone Mapping Spectrometer. Starting points of 24-hour back trajectories were taken over Rome at the bottom, middle, and top heights of the lidar-measured dust layer. Rectangles, built around the endpoints of 24-hour back trajectories, indicate the region where the TAU-initialized dust originated and was subsequently transported over Rome. HYSPLIT transport and dispersion model and READY website (http://www.arl.noaa.gov/ready.html) have been used for computing back trajectories. HYSPLIT was run with the FNL meteorological data archive based on NCEP Global Data Assimilation System (GDAS) model output. Figures 4c, 4e, and 4g relate to 16 May 2001, the day previous to the dust intrusion on 17 May 2001. Figures 4d, 4f, and 4h relate to 11 May 2003, the day previous to the dust intrusion on 12 May 2003.

the forecast errors could sometimes be significant even in cloudless conditions. The technical problems with TOMS measurements explain NASA's decision to replace the calculation of TOMS indices based on the Earth Probe satellite measurements, by OMI indices from the AURA Earth Observing System; this was put into practice from 1 January 2006.

[40] The quantitative comparison at different altitudes showed that the DREAM model predictions are more accurate in the middle part of dust layers than in the top and bottom parts of dust layers.

[41] **Acknowledgments.** This study was supported by the Israeli Ministry of Environment Protection's grant, by the Urban air pollution Italian-Israeli joint project, by the GLOWA-Jordan River BMBF-MOST project, and also by the BMBF-MOST grant 1946 on global change. The authors gratefully acknowledge B. Starobinets and the anonymous reviewers for helpful comments and discussion, and the NOAA Air Resources Laboratory (ARL) for the provision of the HYSPLIT transport and dispersion model and READY website (http://www.arl.noaa.gov/ready.html) used in this publication.

References

Alpert, P., and B. Ziv (1989), The Sharav cyclone: Observations and some theoretical considerations, *J. Geophys. Res.*, *94*, 18,495–18,514.

Alpert, P., B. U. Neeman, and Y. Shay-El (1990), Intermonthly variability of cyclone tracks in the Mediterranean, *J. Clim.*, *3*, 1474–1478.

Alpert, P., S. O. Krichak, M. Tsidulko, H. Shafir, and J. H. Joseph (2002), A dust prediction system with TOMS initialization, *Mon. Weather Rev.*, *130*(9), 2335–2345.

Barkan, J., H. Kutiel, P. Alpert, and P. Kishcha (2004), Investigation of the synoptics of dust intrusion days from the African continent into the Atlantic Ocean, *J. Geophys. Res.*, *109*, D08201, doi:10.1029/2003JD004416.

Barkan, J., P. Alpert, H. Kutiel, and P. Kishcha (2005), The synoptics of dust transportation days from Africa toward Italy and Central Europe, *J. Geophys. Res.*, *110*, D07208, doi:10.1029/2004JD005222.

Barnaba, F., and G. P. Gobbi (2001), Lidar estimation of tropospheric aerosol extinction, surface area and volume: Maritime and desert-dust cases, *J. Geophys. Res.*, *106*(D3), 3005–3018, (Correction: *J. Geophys. Res., 107*(D13), 4180, doi:10.1029/2002JD002340, 2002).

Bergametti, G., A. L. Dutot, P. Buat-Menard, R. Losno, and E. Remoudaki (1989), Seasonal variability of the elemental composition of atmospheric aerosol particles over the northwestern Mediterranean, *Tellus, Ser. B*, *41*, 353–361.

Ginoux, P., M. Chin, I. Tegen, J. M. Prospero, B. Holben, O. Dubovik, and S.-J. Lin (2001), Sources and distributions of dust aerosols simulated with the GOCART model, *J. Geophys. Res.*, *106*, 20,255–20,274.

Gobbi, G. P., F. Barnaba, M. Blumthaler, G. Labow, and J. Herman (2002), Observed effects of particles non-sphericity on the retrieval of marine and desert-dust aerosol optical depth by lidar, *Atmos. Res.*, *61*, 1–14.

Gobbi, G. P., F. Barnaba, R. Van Dingenen, R. Putaud, M. Mircea, and M. C. Facchini (2003), Lidar and in situ observations of continental and Saharan aerosol: Closure analysis of particles optical and physical properties, *Atmos. Chem. Phys.*, *3*, 2161–2172.

Gobbi, G. P., F. Barnaba, and L. Ammannato (2004), The vertical distribution of aerosols, Saharan dust and clouds at Rome (Italy) in the year 2001, *Atmos. Chem. Phys.*, *3*, 2161–2172.

Janjic, Z. I. (1994), The step-mountain Eta coordinate model: Further developments of the convection, viscous sublayer and turbulence closure schemes, *Mon. Weather Rev.*, *122*, 927–945.

Kallos, G., et al. (1997), The regional weather forecasting system SKIRON: An overview, in *Proceedings of Symposium on Regional Weather Prediction on Parallel Computer Environments*, edited by G. Kallos, V. Kotroni, and K. Lagouvardos, Univ. of Athens, Athens, ISBN:960-8468-22-1.

Kallos, G., P. Katsafados, A. Papadopoulos, and S. Nickovic (2006), Transatlantic Saharan dust transport: Model simulation and results, *J. Geophys. Res.*, *111*, D09204, doi:10.1029/2005JD006207.

Kaufman, Y. J., D. Tanre, and O. Boucher (2002), A satellite view of aerosols in the climate system, *Nature*, *419*, 215–223.

Kinne, S., et al. (2003), Monthly averages of aerosol properties: A global comparison among models, satellite data and AERONET ground data, *J. Geophys. Res.*, *108*(D20), 4634, doi:10.1029/2001JD001253.

Kishcha, P., F. Barnaba, G. P. Gobbi, P. Alpert, A. Shtivelman, S. O. Krichak, and J. H. Joseph (2005), Vertical distribution of Saharan dust over Rome (Italy): Comparison between 3-year model predictions and lidar soundings, *J. Geophys. Res.*, *110*, D06208, doi:10.1029/2004JD005480.

Krichak, S. O., P. Alpert, and A. Shtivelman (2003), First results of investigation of radiative effects of mineral dust in an atmospheric model with optimized dust source determination, Session AS14, EGS-AGU-EUG Joint Assembly, Nice, France, 6–11 April.

Moulin, C., et al. (1998), Satellite climatology of African dust transport in the Mediterranean atmosphere, *J. Geophys. Res.*, *103*, 13,137–13,144.

Nickovic, S. (2005), Distribution of dust mass over particle sizes: Impacts on atmospheric optics, paper presented at Fourth ADEC Workshop: Aeolian Dust Experiment on Climate Impact, Jpn. Meteorol. Agency, Nagasaki, Japan, 26–28 Jan.

Nickovic, S., and S. Dobricic (1996), A model for long-range transport of desert dust, *Mon. Weather Rev.*, *124*, 2537–2544.

Nickovic, S., G. Kallos, O. Kakaliagou, and D. Jovic (1997), Aerosol production/transport/deposition processes in the Eta model: Desert cycle simulations, in *Proceedings of the Symposium on Regional Weather Prediction on Parallel Computer Environments*, edited by G. Kallos, V. Kotroni, and K. Lagouvardos, pp. 137–145, Univ. of Athens, Athens.

Nickovic, S., G. Kallos, A. Papadopoulos, and O. Kakaliagou (2001), A model for prediction of desert dust cycle in the atmosphere, *J. Geophys. Res.*, *106*, 18,113–18,129.

Nickovic, S., G. Pejanovic, E. Ozsoy, C. Pérez, and J. M. Baldasano (2004), Interactive radiation-dust model: A step to further improve weather forecasts, paper presented at International Symposium on Sand and Dust Storm, World Meteorol. Org., Beijing, China, 12–14 September.

Papadopoulos, A. (2001), A limited area model with specific capabilities to handle initial and boundary conditions, Ph.D. thesis, 263 pp., School of Physics, Univ. of Athens, Athens.

Papadopoulos, A., G. Kallos, S. Nickovic, D. Jovic, M. Dacic, P. Katsafados (1997), Sensitivity studies of the surface and radiation parameterization schemes of the SKIRON system, in *Proceedings of Symposium on Regional Weather Prediction on Parallel Computer Environments*, edited by G. Kallos, V. Kotroni, and K. Lagouvardos, pp. 155–164, Univ. of Athens, Athens, ISBN:960-8468-22-1.

Pérez, C., S. Nickovic, G. Pajanovic, J. M. Baldasano, and E. Ozsoy (2006a), Interactive dust-radiation modeling: A step to improve weather forecasts, *J. Geophys. Res.*, *111*, D16206, doi:10.1029/2005JD006717.

Pérez, C., S. Nickovic, J. M. Baldasano, M. Sicard, F. Rocadenbosch, and V. E. Cachorro (2006b), A long Saharan dust event over the western Mediterranean: Lidar, sun photometer observations and regional dust modeling, *J. Geophys. Res.*, *111*, D15214, doi:10.1029/2005JD006579.

Ramanathan, V., P. J. Crutzen, J. T. Kiehl, and D. Rosenfeld (2001), Aerosols, climate, and the hydrological cycle, *Science*, *294*, 2119–2124.

Rosenfeld, D. (2002), Suppression of rain and snow by urban and industrial air pollution, *Science*, *287*, 1793–1796.

Shao, Y., M. R. Raupach, and P. A. Findlater (1993), Effects of saltation bombardment on the entrainment of dust by wind, *J. Geophys. Res.*, *98*, 12,719–12,726.

P. Alpert, J. H. Joseph, P. Kishcha, S. O. Krichak, and A. Shtivelman, Department of Geophysics and Planetary Sciences, Tel Aviv University, 69978 Tel Aviv, Israel. (kishcha@gmail.com)

J. M. Baldasano and C. Pérez, Earth Sciences Department, Barcelona Supercomputing Center, 08034 Barcelona, Spain.

F. Barnaba, Climate Change Unit, Institute for Environment and Sustainability, Joint Research Centre (JRC), European Commission, I-21020 Ispra (VA), Italy.

G. P. Gobbi, Istituto di Scienze dell'Atmosfera e del Clima, Italian National Research Council (CNR), 00133 Rome, Italy.

G. Kallos, P. Katsafados, and C. Spyrou, Division of Environment, School of Physics, University of Athens, 15784 Athens, Greece.

S. Nickovic, Atmospheric Research and Environment Programme, World Meteorological Organization, CH 1211, Geneva 2, Switzerland.